

MODELING ARSENATE COMPETITIVE ADSORPTION ON KAOLINITE, MONTMORILLONITE AND ILLITE

BRUCE A. MANNING AND S. GOLDBERG

USDA-ARS, U.S. Salinity Laboratory, 450 West Big Springs Road, Riverside, California 92507

Abstract—The adsorption of arsenate (As(V)) on kaolinite, montmorillonite and illite was investigated at varying pH and competing anion concentration while holding As(V) concentration ($6.7 \times 10^{-7} M$), clay suspension density (2.5 g L^{-1}) and ionic strength ($0.1 M \text{ NaCl}$) constant. The effects of 2 concentrations of phosphate (P) or molybdate (Mo) (6.7×10^{-7} and $6.7 \times 10^{-6} M$) on As(V) adsorption envelopes (adsorption vs. pH) gave evidence for direct competitive adsorption (in the case of As(V) + P) and possibly site-specific non-competitive adsorption (As(V) + Mo). Distinct As(V) adsorption maxima occurred at approximately pH 5.0 for kaolinite, 6.0 for montmorillonite and 6.5 for illite, and ranged from 0.15 to 0.22 mmol As(V) kg^{-1} . When both As(V) and P were present at equimolar concentrations ($6.7 \times 10^{-7} M$), As(V) adsorption decreased slightly, whereas As(V) adsorption substantially decreased in binary As(V)/P systems when the P concentration was $6.7 \times 10^{-6} M$, which was 10 times greater than As(V). The presence of Mo at equimolar ($6.7 \times 10^{-7} M$) and 10 times greater ($6.7 \times 10^{-6} M$) concentrations than As(V) caused only slight decreases in As(V) adsorption because the Mo adsorption maximum occurred at $\text{pH} < 4$. The constant capacitance surface complexation model was applied to As(V) and P adsorption data and was used to predict As(V) adsorption at varying P concentrations. The model gave reasonable descriptions of As(V) adsorption on the 3 clay minerals at varying pH and in the presence of a competing oxyanion (P), indicating that surface complexation modeling may be useful in predicting As(V) adsorption in soils.

Key Words—Arsenate competitive adsorption, Illite, Kaolinite, Montmorillonite.

INTRODUCTION

Arsenic (As) is a toxic contaminant that can be found in both anthropogenic wastes and some geochemical environments. The most stable species of As in oxidizing environments is arsenate (As(V)) (Sadiq et al. 1983), though microbial reduction of As(V) to As(III) (Masscheleyn et al. 1991a, 1991b) and transformations of inorganic As to organic, methylated forms (Ferguson and Gavis 1972) can occur under certain conditions. Arsenate exists in solution as the pH-dependent deprotonated oxyanions of arsenic acid (H_2AsO_4^- , HAsO_4^{2-} and AsO_4^{3-}). In soils, As(V) is retained by adsorption, the magnitude of which is dependent upon several factors including pH (Goldberg and Glaubig 1988), competing anion concentrations (Roy et al. 1986), and Fe and Al oxide content (Jacobs et al. 1970).

Numerous studies have investigated As(V) adsorption on Fe and Al oxide minerals including high defect hydrous Fe and Al oxides (Anderson and Malotky 1979), goethite and gibbsite (Hingston et al. 1971, 1972; Goldberg 1986) and ferrihydrite (Waychunas et al. 1993). The adsorption of As(V) in soils is significantly correlated with ammonium oxalate-extractable Al and Fe (Jacobs et al. 1970; Livesey and Huang 1981) and hence, determining the mechanism of As(V) binding to FeOH and AlOH surface hydroxyl groups is of importance. Direct evidence for the formation of inner-sphere As(V) adsorption complexes on a variety of Fe oxides has been provided by extended X-ray

absorption fine structure (EXAFS) spectra (Waychunas et al. 1993), on hydrous Fe oxide by energy dispersive analysis of X-rays (EDAX) (Hsia et al. 1994) and on goethite by infrared spectroscopy (Lumsdon et al. 1984). Indirect evidence for inner-sphere adsorption of As(V) on amorphous Fe and Al oxides has also been provided by point of zero charge (PZC) shifts from electrophoretic mobility measurements (Anderson and Malotky 1979).

Relatively few studies have focused on As(V) adsorption on well-characterized phyllosilicate clay minerals. Moreover, factors that affect As(V) adsorption on phyllosilicates including pH and competing anions are not well understood. Frost and Griffin (1977) investigated As(V), As(III) and Se(IV) adsorption from landfill leachate on montmorillonite and kaolinite and concluded that pH-dependent As(V) adsorption was due to preferential adsorption of the H_2AsO_4^- species. The adsorption of As(V) on kaolinite has been shown to depend on both solution speciation of As(V) and surface charge (Xu et al. 1988). Huang (1975) concluded that As(V) adsorbed on hydroxy-Al on the external surfaces but not in the interlamellar region of biotite and vermiculite. The proposed sites of anion adsorption on layer silicates are positively charged AlOH_2^+ functional groups at exposed crystal edges (Muljadi et al. 1966; Swartzen-Allen and Matijevic 1974; Keren and Talpaz 1984). Also, charged FeOH_2^+ functional groups from isomorphic substitution of Fe for Al may be of minor importance for montmorillonite

Table 1. Numerical input values and intrinsic surface complexation constants for As(V) and P adsorption on kaolinite (KGa-1), montmorillonite (SWy-1), and illite (IMt-2) optimized using the constant capacitance model.

Capacitance density ($F\ m^{-2}$)	1.06		
	2.5		
Suspension density ($g\ L^{-1}$)	0.1 M NaCl		
Background electrolyte	KGa-1	SWy-1	IMt-2
BET surface area ($m^2\ g^{-1}$)	9.1	18.6	24.2
Site density ($\times 10^{-6}$ mol sites g^{-1}) [†]	2.44	1.11	1.16
$\log K_+(int)$ [‡]	6.40	6.09	6.00
$\log K_-(int)$	-10.4	-10.2	-10.5
$\log K_{As}^1(int)$	10.0	8.52	9.24
$\log K_{As}^2(int)$	2.96	3.65	3.66
$\log K_{As}^3(int)$	-4.55	-4.18	-4.35
$V_{As(V)}$ [§]	1.11	1.06	0.84
$\log K_P^1(int)$	10.6	NC#	8.30
$\log K_P^2(int)$	3.66	4.12	3.38
$\log K_P^3(int)$	-4.88	-4.03	-5.98
V_P	5.27	5.77	10.1

[†] Site densities used in constant capacitance modeling were derived from maximum anion adsorption densities.

[‡] All intrinsic surface complexation constants were calculated as $mol\ L^{-1}$.

[§] $V_{As(V)}$ = goodness of fit parameter for As(V) (see Eq. 14).

NC = no convergence.

ite. Direct spectroscopic evidence for the formation of inner-sphere complexes between oxyanions and the Al^{3+} cation at the phyllosilicate crystal edge site is not yet available.

Attempts to elucidate the mechanisms of oxyanion adsorption on clay minerals have included studies on the effects of competing anions and chemical modeling. Phosphate (P) adsorption on kaolinite, montmorillonite and illite is insensitive to the presence of both SO_4^{2-} and Cl^- (Edzwald et al. 1976), whereas organic anions decrease the adsorption of P (Chen et al. 1973a) and As(V) (Xu et al. 1988) on kaolinite. Zachara et al. (1988) suggested that the independent adsorption of CrO_4^{2-} and SO_4^{2-} on kaolinite was due to site-specific adsorption of the 2 anions arising from the complex, nonhomogeneous structure of the kaolinite edge. The triple-layer surface complexation model used by Zachara et al. (1988) adequately described CrO_4^{2-} adsorption on kaolinite between pH 5.0 and 7.5 by assuming the formation of pH-dependent outer-sphere $AlOH_2^+-CrO_4^{2-}$ and $AlOH_2^+-HCrO_4^-$ surface complexes. The constant capacitance model (Stumm et al. 1970; Schindler and Gamsjäger 1972; Stumm et al. 1976; Stumm et al. 1980) has been used successfully to describe molybdate (Mo) adsorption isotherms on kaolinite, montmorillonite and illite (Motta and Miranda 1989).

The intention of this study was to investigate the effects of pH, P and Mo on the adsorption of As(V) on kaolinite, montmorillonite and illite. Phosphate and Mo were chosen as competing oxyanions because, like

As(V), they are tetrahedral and adsorb on Fe and Al oxides by an inner-sphere mechanism (Hingston et al. 1971, 1972; Bleam et al. 1991). The constant capacitance model (CCM) was used to calculate intrinsic equilibrium constants ($K(int)$) for As(V) and P adsorption on clays in single ion adsorption experiments. In the binary As(V)/P systems, the CCM was used to predict competitive As(V) adsorption on clay minerals using $K(int)$ values optimized in single ion systems. This procedure was not applied to the As(V)/Mo binary system because Mo displayed adsorption characteristics that were different from As(V) and P and competitive adsorption was less pronounced. Determining intrinsic surface complexation constants for As(V) adsorption on clay minerals under controlled conditions will be useful for predicting the mobility of As(V) in soils that contain mixtures of clay minerals.

EXPERIMENTAL

Clay Mineral Characterization

The clay minerals used in this study were obtained from the Clay Minerals Society Source Clay Minerals Repository. Wyoming montmorillonite (SWy-1) and Georgia kaolinite (KGa-1) were used without further preparation. Montana illite (IMt-2) fragments were ground with a mortar and pestle to pass a $<500\ \mu m$ sieve. It was the intention of this study to use the source clay materials with a minimum of pretreatment to preserve their natural mineralogy. Impurities such as Fe and Al oxide coatings would enhance oxyanion adsorption on these materials, however, the adsorption capacities of the clay minerals was approximately 2 orders of magnitude less than pure crystalline goethite (α -FeOOH) and gibbsite (γ -Al(OH)₃) (Manning and Goldberg 1996) suggesting that Fe and Al coatings were at most minor constituents. Clay characterization included XRD analyses of both random powder mounts and oriented slide mounts. The kaolinite used in this study contained trace impurities of feldspar and vermiculite. Montmorillonite showed a trace impurity of mica and illite was X-ray pure. Specific surface areas of the clay sorbents were determined by single-point Brunauer-Emmett-Teller (BET) N_2 adsorption with a Quantisorb Jr. surface area analyzer (Quantachrome Corporation, Syosset, NY) and are given in Table 1.

As(V), P and Mo Analyses

All As(V) analyses were performed by hydride generation atomic absorption spectrophotometry (HGAAS) with a Perkin Elmer 3030B atomic absorption spectrophotometer equipped with an externally-powered arsenic electrodeless discharge lamp operating at 8 watts. Standard solutions of $Na_2HAsO_4 \cdot 7H_2O$ in 0.1 M NaCl were used for instrument calibration ($\lambda = 193.7\ nm$, slit = 0.7). The hydride (arsine, AsH_3) was produced with a continuous flow Varian vapor

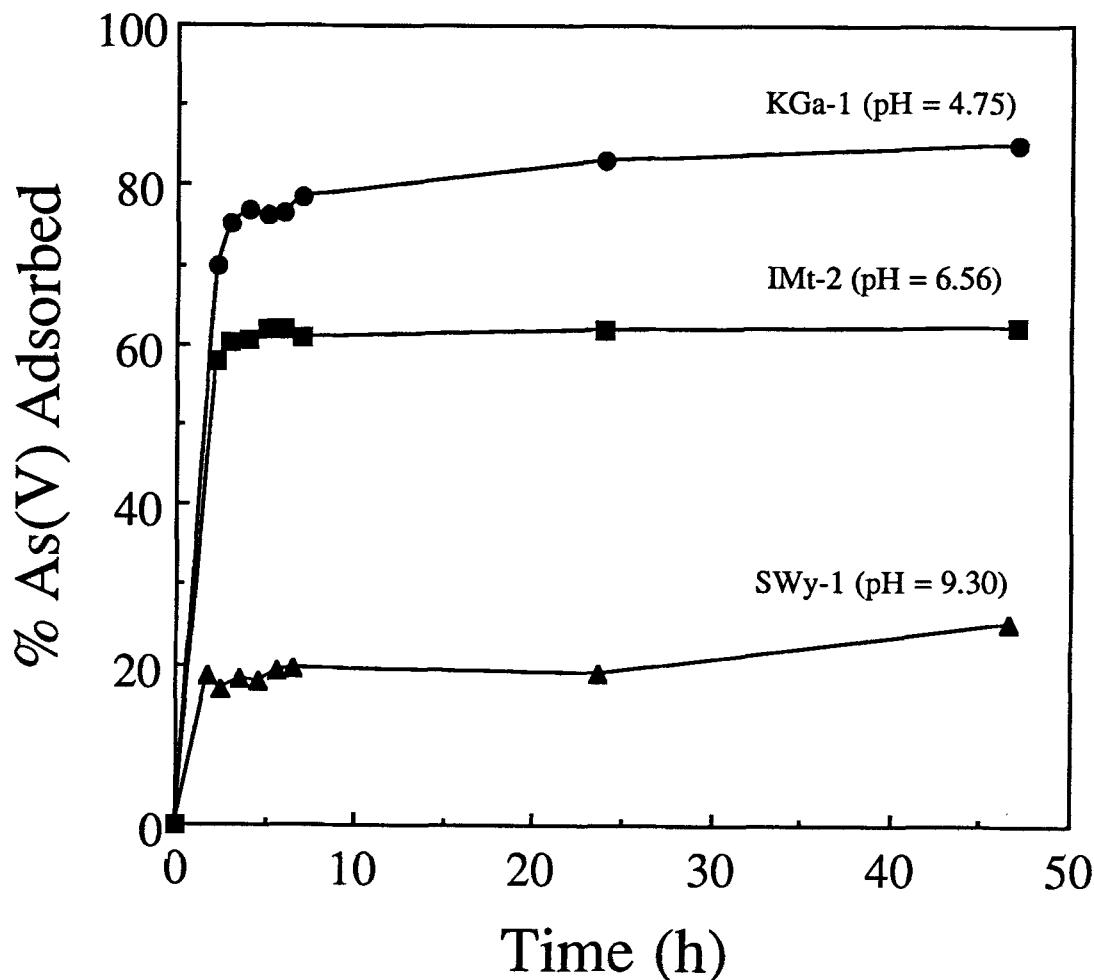


Figure 1. Arsenate adsorption on kaolinite (KGa-1), montmorillonite (SWy-1) and illite (IMt-2) as a function of time. Initial As(V) concentration = $0.67 \mu\text{M}$, suspension density = 2.5 g L^{-1} , and background electrolyte = 0.1 M NaCl .

generation accessory (VGA-76) by reacting sample solutions with $0.16 \text{ M NaBH}_4/0.12 \text{ M NaOH}$ and 10 M HCl . The linear analytical range for the instrument was 0 to $0.7 \mu\text{M As(V)}$ and the detection limit was $7.0 \times 10^{-9} \text{ M As(V)}$ ($0.5 \mu\text{g As(V)L}^{-1}$).

Phosphate was determined using a Dionex 2000 ion chromatograph (IC) (Dionex Corporation, Sunnyvale, CA) with an OmniPac PAX-500 column ($4.6 \times 250 \text{ mm}$), an eluent (15 mM NaOH) flow rate of 0.75 mL min^{-1} , and suppressed ion conductivity detection interfaced with a Hewlett Packard 3390 reporting integrator. Average P retention time was 6.9 min . Prior to IC analyses, chloride was removed from sample solutions with Dionex On-guard Ag solid phase extraction columns ($7 \times 5 \text{ mm ID}$). Molybdenum was analyzed by inductively coupled plasma emission spectrometry. Sample solutions were diluted by $\frac{1}{2}$ with $2\% \text{ HNO}_3$ to make the final matrix 0.05 M NaCl in $1\% \text{ HNO}_3$.

Adsorption Envelope Experiments

Adsorption envelopes (anion adsorption vs. suspension pH) were produced as batch reactions in 40 mL polycarbonate centrifuge tubes. In single anion systems, 50 mg of clay sorbent was reacted with 20 mL of $0.67 \mu\text{M As(V)}$ in 0.1 M NaCl . Binary (dual adsorbate) systems contained $0.67 \mu\text{M As(V)}$ and either 0.67 or $6.7 \mu\text{M}$ competing anion (P or Mo). Stock solutions of P and Mo were produced from the Na salts ($\text{NaH}_2\text{PO}_4 \cdot \text{H}_2\text{O}$ and $\text{Na}_2\text{MoO}_4 \cdot 2\text{H}_2\text{O}$) and pH was adjusted with 0.1 M NaOH or HCl . The tubes were shaken for 20 h at room temperature ($22 \pm 1 \text{ }^\circ\text{C}$) on a reciprocating shaker ($120 \text{ oscillations min}^{-1}$) and centrifuged at $12,500 \times g$ for 10 min . Supernatant pH was measured with a Thomas glass combination pH electrode and a Beckman potentiometer followed by filtering with $0.45 \mu\text{m}$ Whatman cellulose nitrate

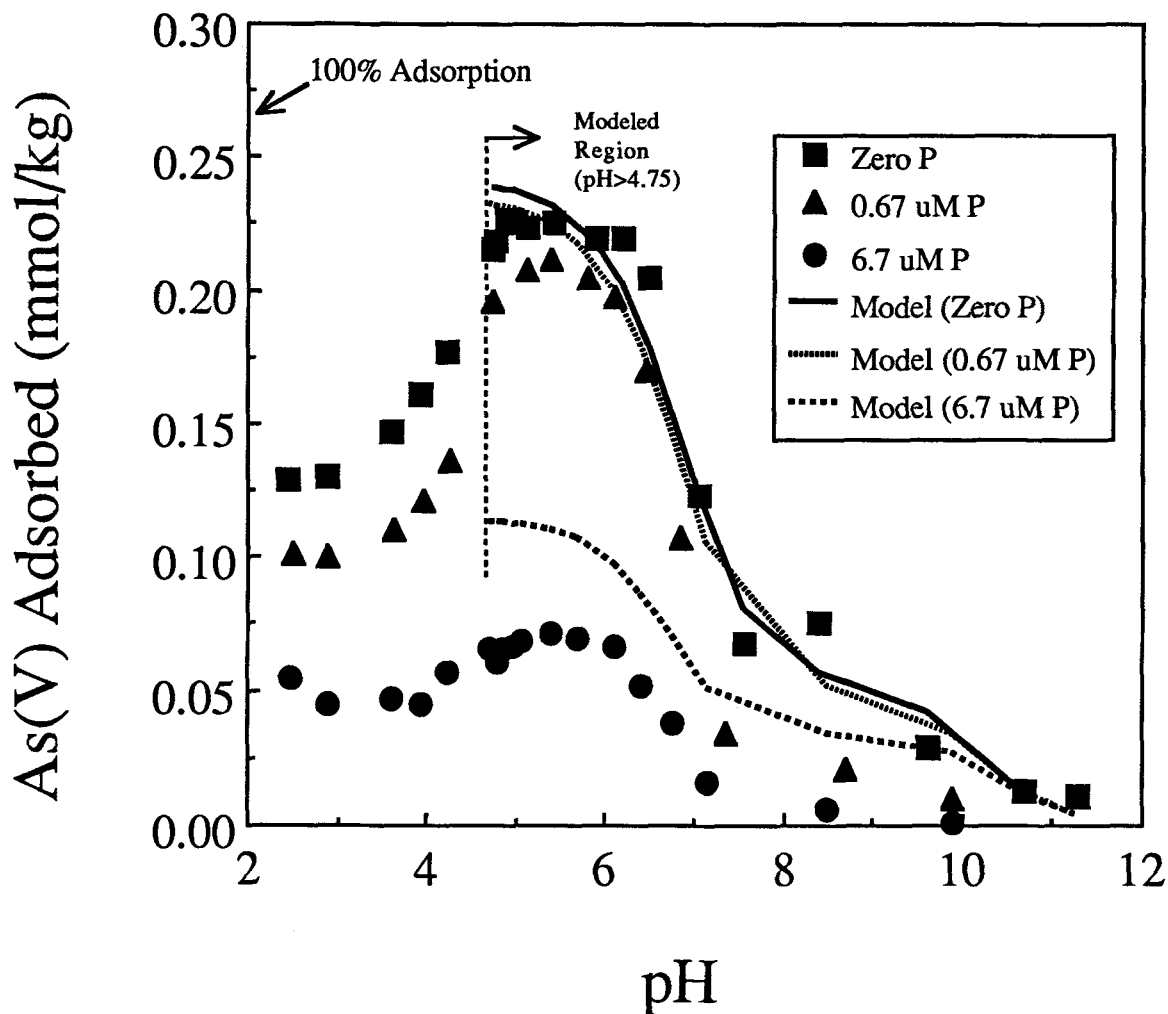


Figure 2. Experimental (points) and model (lines) As(V) adsorption envelopes on kaolinite (KGa-1) at varying phosphate concentrations. Five adjustable $K(\text{int})$ parameters were optimized to fit the CCM to single As(V) anion data (solid line), whereas the $K(\text{int})$ values were held constant to predict competitive adsorption in binary systems (dotted lines). Initial As(V) concentration = $0.67 \mu\text{M}$, suspension density = 2.5 g L^{-1} , background electrolyte = 0.1 M NaCl , and reaction time = 20 h.

membranes. Solution As(V) was then analyzed by HGAAS and adsorbed As(V) was calculated as the difference between the concentration before and after equilibration with the solids.

Two preliminary experiments were performed to characterize the As(V)/clay mineral systems. The time course of As(V) adsorption on the 3 clay minerals in unbuffered 0.1 M NaCl was determined at 2, 3, 4, 5, 6, 7, 24 and 48 h. Based on these data (Figure 1), 20 h was determined to be adequate time for equilibration. The possibility of As(V) reduction to As(III) was investigated by analyzing supernatants for As(III) after equilibration with clays using the oxalate buffer/HGAAS method of Glaubig and Goldberg (1988). No As(III) was detectable under the reaction conditions used in this study.

Constant Capacitance Modeling

The CCM was used to calculate $K(\text{int})$ values for As(V) and P adsorption on clays in single anion systems. Constants for As(V) and P adsorption that were optimized in single ion systems were used to predict competitive adsorption in binary anion systems. The model is based on the following assumptions: 1) ion adsorption occurs by an inner-sphere ligand exchange mechanism; 2) no surface complexes are formed with ions in the background electrolyte; and 3) the net surface charge, σ_o ($\text{mol}_e \text{ L}^{-1}$), is a linear function of the surface potential, Ψ_o (volts):

$$\sigma_o = (CS_A M_v / F) \Psi_o \quad [1]$$

where subscript o refers to the surface, C (Fm^{-2}) is the capacitance density at the surface, S_A ($\text{m}^2 \text{g}^{-1}$) is

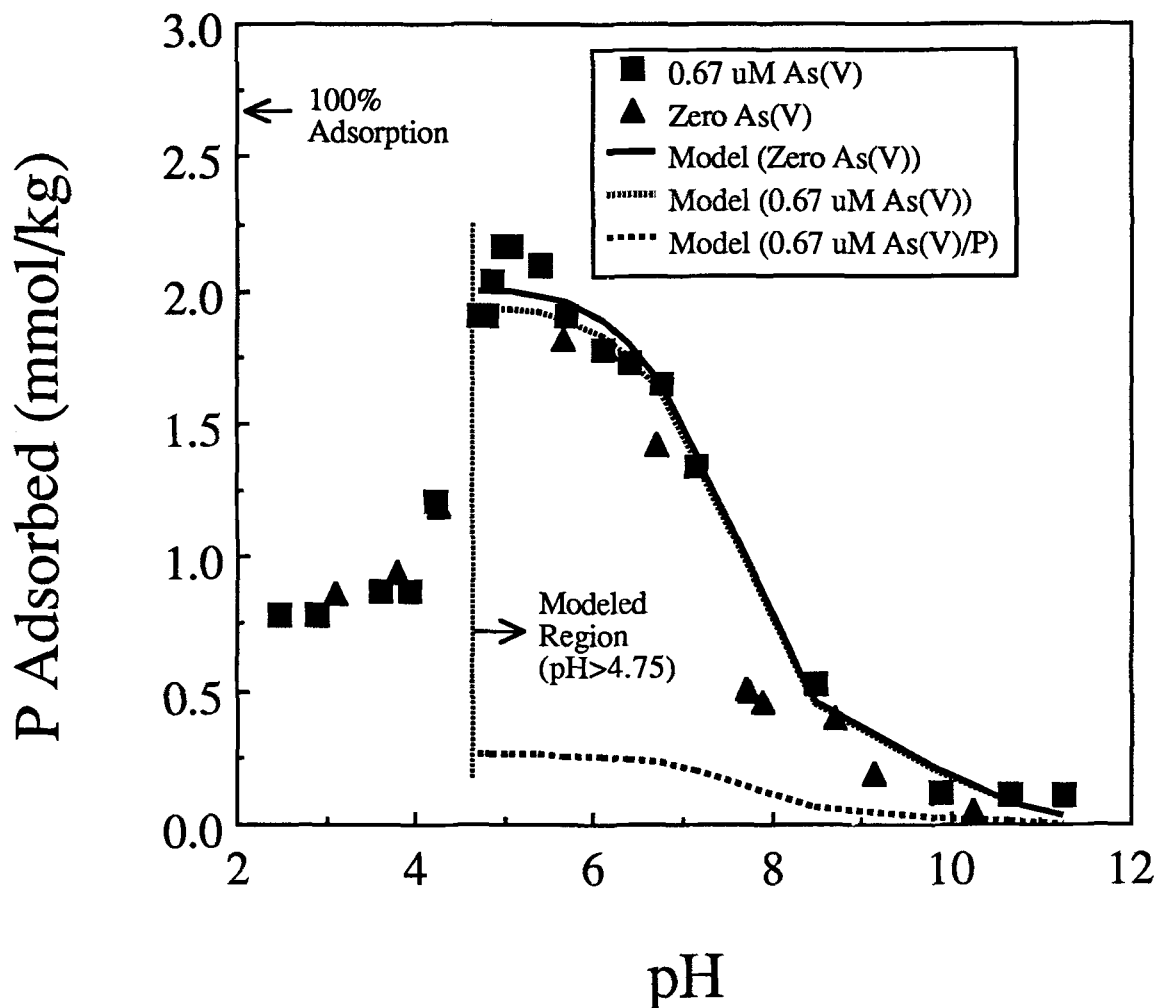
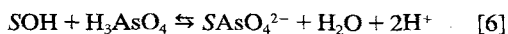
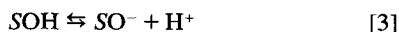
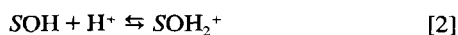


Figure 3. Experimental (points) and model (lines) P adsorption envelopes on kaolinite (KGa-1) in the presence and absence of As(V). Five adjustable $K(\text{int})$ parameters were optimized to fit the CCM to single P anion data (solid line), whereas the $K(\text{int})$ values were held constant to predict competitive adsorption in binary systems (dotted lines). Reaction conditions: anion concentrations = $6.7 \mu\text{M P}/0.67 \mu\text{M As(V)}$ (binary system) or $6.7 \mu\text{M P}$ (single ion system), clay suspension density = 2.5 g L^{-1} , 0.1 M NaCl , and reaction time = 20 h. The lowest dashed line is a model prediction of P adsorption in the binary $0.67 \mu\text{M As(V)}/0.67 \mu\text{M P}$ system (no experimental data).

the specific surface area, M_v (g L^{-1}) is the suspension density of the solid and F (9.65×10^{-4} coulombs mol^{-1}) is the Faraday constant. The capacitance density, C , was fixed at 1.06 F m^{-2} which was the optimal value for $\gamma\text{-Al}_2\text{O}_3$ (Westall and Hohl 1980).

The CMM uses the following set of reactions to calculate monodentate specific adsorption of As(V) on the oxide surface:



where SOH is defined as 1 mol of reactive hydroxyl groups on the oxide surface. The equivalent set of expressions could be written for H_2PO_4 by replacing As with P in Equations [4] through [6]. Bidentate anion surface complexes were not considered in this study due to: 1) a lack of direct experimental evidence for their formation on clay mineral edges; and 2) our efforts to keep the number of adjustable parameters in the CCM to a minimum. Solution complexes such as $\text{AlH}_2\text{AsO}_4^{2+}$ and AlHAsO_4^+ were also not considered in this study.

The reactions in Equations [4] through [6] are written such that model components are the reactants that form model species as products. Components are defined in the CCM as fundamental entities from which all species are derived. The components used for the case of As(V) single-anion adsorption were SOH, H_3AsO_4 , H^+ and P_0 .

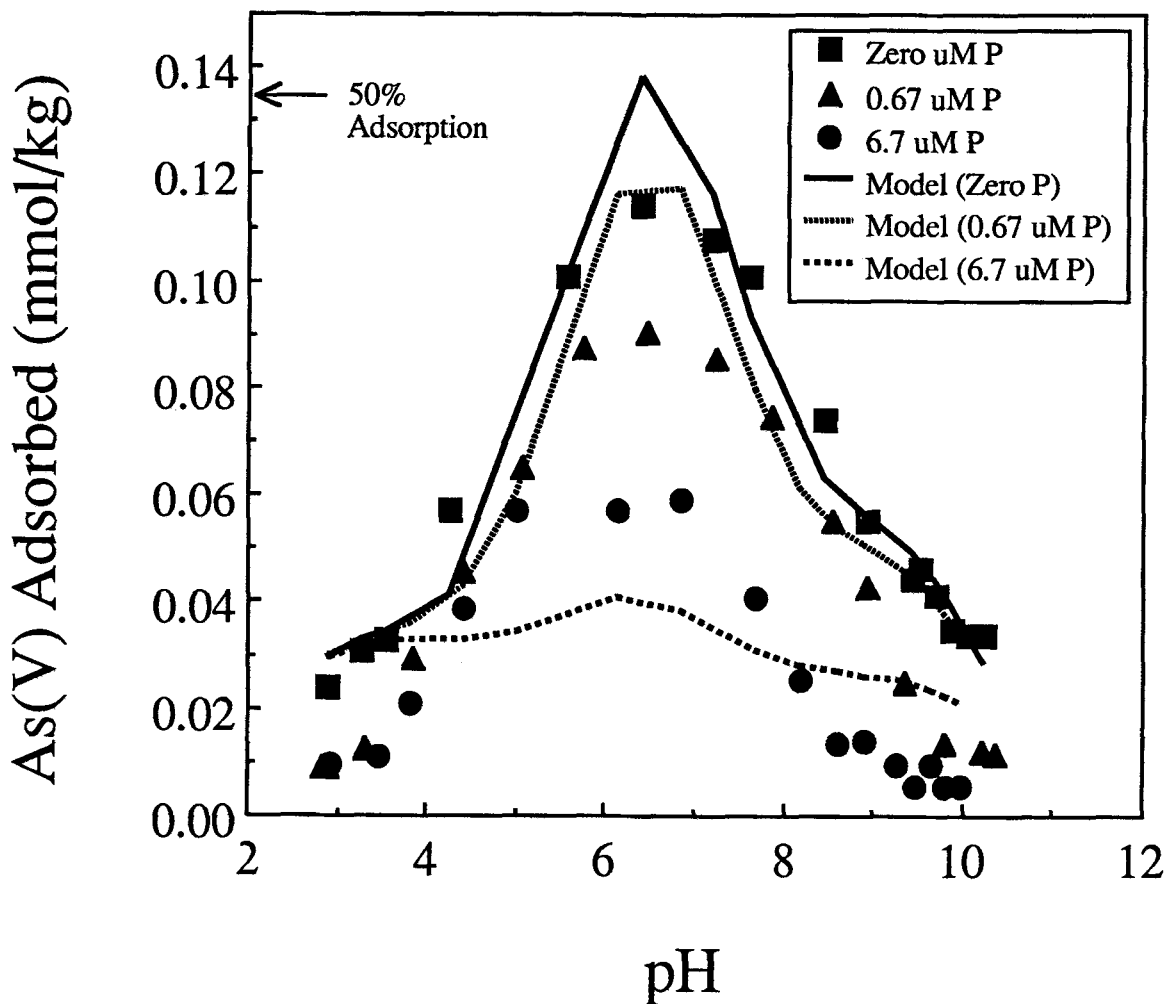


Figure 4. Experimental (points) and model (lines) As(V) adsorption envelopes on montmorillonite (SWy-1) at varying P concentrations. Five adjustable $K(\text{int})$ parameters were optimized to fit the CCM to single As(V) anion data (solid line), whereas the $K(\text{int})$ values were held constant to predict competitive adsorption in binary systems (dotted lines). Initial As(V) concentration = $0.67 \mu\text{M}$, suspension density = 2.5 g L^{-1} , background electrolyte = 0.1 M NaCl , and reaction time = 20 h.

Equations [4] through [6] are not necessarily the true reactions that occur at the surface, but are written so as to form species, for example, SOH_2^+ , SAsO_4^{2-} , only from components. The intrinsic equilibrium constants for the reactions in Equations [2] through [6] are:

$$K_{\text{S}^-}(\text{int}) = \frac{[\text{SOH}_2^+]}{[\text{SOH}][\text{H}^+]} \exp(F\Psi_o/RT) \quad [7]$$

$$K_{\text{S}^-}(\text{int}) = \frac{[\text{SO}^-][\text{H}^+]}{[\text{SOH}]} \exp(-F\Psi_o/RT) \quad [8]$$

$$K_{\text{SAs}}^1(\text{int}) = \frac{[\text{SH}_2\text{AsO}_4]}{[\text{SOH}][\text{H}_3\text{AsO}_4]} \quad [9]$$

$$K_{\text{SAs}}^2(\text{int}) = \frac{[\text{SHAsO}_4^-][\text{H}^+]}{[\text{SOH}][\text{H}_3\text{AsO}_4]} \exp(-F\Psi_o/RT) \quad [10]$$

$$K_{\text{SAs}}^3(\text{int}) = \frac{[\text{SAsO}_4^{2-}][\text{H}^+]^2}{[\text{SOH}][\text{H}_3\text{AsO}_4]} \exp(-2F\Psi_o/RT) \quad [11]$$

where R is the molar universal gas constant and T is the absolute temperature (K). The mass balance and charge balance equations for the surface hydroxyl group are given by:

$$\begin{aligned} [\text{SOH}]_T &= [\text{SOH}] + [\text{SOH}_2^+] + [\text{SO}^-] \\ &\quad + [\text{SH}_2\text{AsO}_4] + [\text{SHAsO}_4^-] \\ &\quad + [\text{SAsO}_4^{2-}] \end{aligned} \quad [12]$$

$$\begin{aligned} \sigma_o &= [\text{SOH}_2^+] - [\text{SO}^-] \\ &\quad - [\text{SHAsO}_4^-] - 2[\text{SAsO}_4^{2-}] \end{aligned} \quad [13]$$

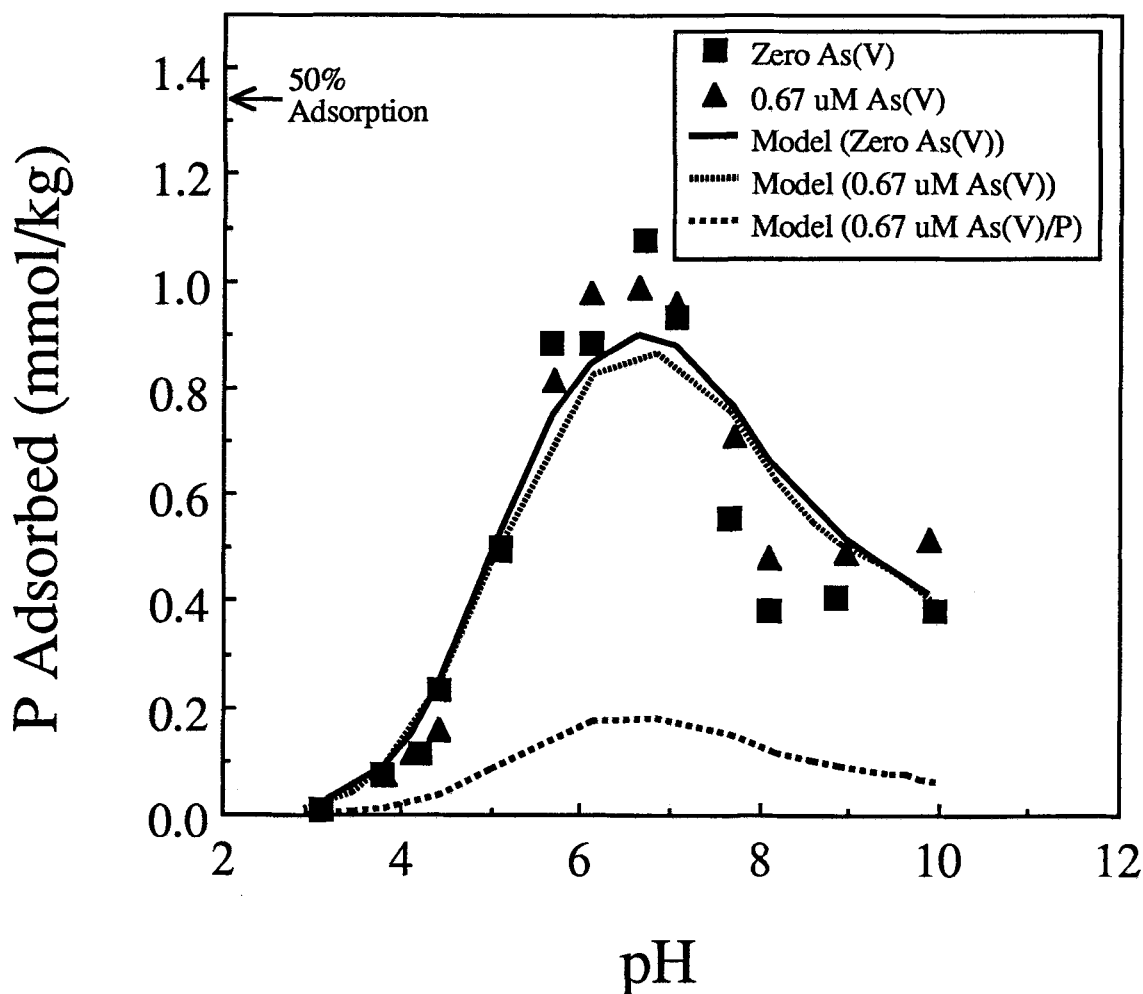


Figure 5. Experimental (points) and model (lines) P adsorption envelopes on montmorillonite (SWy-1) in the presence and absence of As(V). Five adjustable $K(\text{int})$ parameters were optimized to fit the CCM to single P anion data (solid line), whereas the $K(\text{int})$ values were held constant to predict competitive adsorption in binary systems (dotted lines). Reaction conditions: anion concentrations = $6.7 \mu\text{M P}/0.67 \mu\text{M As(V)}$ (binary system) or $6.7 \mu\text{M P}$ (single ion system), clay suspension density = 2.5 g L^{-1} , 0.1 M NaCl , and reaction time = 20 h. The lowest dashed line is a model prediction of P adsorption in the binary $0.67 \mu\text{M As(V)}/0.67 \mu\text{M P}$ system (no experimental data).

The computer program FITEQL 3.1 (Herbelin and Westall 1994) was used to solve the set of Equations [7] to [13]. The FITEQL program iteratively optimizes a chosen set of $K(\text{int})$ by minimizing the differences between calculated and experimental adsorption data using a nonlinear least squares optimization routine. The goodness-of-fit parameter (V_Y) in FITEQL is defined as the overall variance in Y (weighted sum of squares divided by degrees of freedom)

$$V_Y = \frac{\sum (Y_i/s_i)^2}{(n_p n_c) - n_a} \quad [14]$$

where Y_i is the residual for each adsorption envelope data point i , s_i is the error estimate, n_p is the number of data points in the adsorption envelope, n_c is the

number of system components for which both the total and free concentrations are known and n_a is the number of adjustable parameters in the system (Herbelin and Westall 1994). Five adjustable parameters ($K(\text{int})$ values) were used to fit As(V) and P single anion adsorption data. The values of V_Y and the optimized $K(\text{int})$ values for As(V) and P adsorption systems are given in Table 1 along with numerical input values.

A set of intrinsic surface protonation ($K_+(\text{int})$) and deprotonation ($K_-(\text{int})$) constants were optimized in both As(V) and P ion systems for each clay. The final values of $K_+(\text{int})$ and $K_-(\text{int})$ used (Table 1) were derived by checking values of $K_+(\text{int})$ and $K_-(\text{int})$ intermediate between those optimized in the As(V) and P systems for goodness of fit in FITEQL. During the final optimization of the sets of single anion $K_{SAs}(\text{int})$

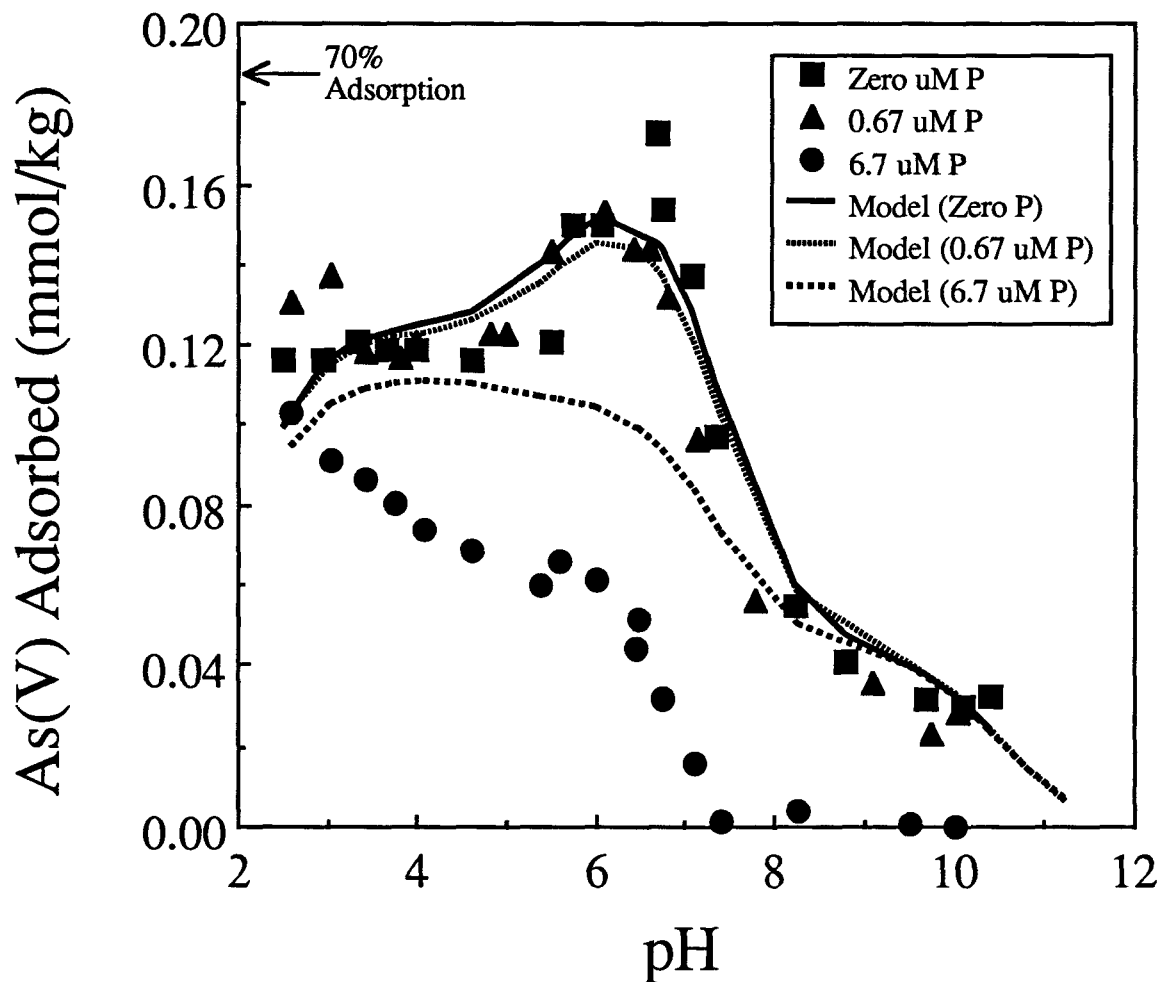


Figure 6. Experimental (points) and model (lines) As(V) adsorption envelopes on illite (IMt-2) at varying P concentrations. Five adjustable K_{int} parameters were optimized to fit the CCM to single As(V) anion data (solid line), whereas the K_{int} values were held constant to predict competitive adsorption in binary systems (dotted lines). Initial As(V) concentration = $0.67 \mu\text{M}$, suspension density = 2.5 g L^{-1} , background electrolyte = 0.1 M NaCl , and reaction time = 20 h.

and $K_{\text{sp}}(\text{int})$ in FITEQL, the intermediate $K_{+}(\text{int})$ and $K_{-}(\text{int})$ values were held constant. When modeling competitive adsorption between As(V) and P in binary anion systems, all 5 adjustable parameters were held constant and thus are referred to as predictions. This procedure gave the best fit of the model to the experimental data and allowed an indirect estimate of the point of zero charge of the clay mineral edges (PZC_{edge}) from the equation:

$$\text{PZC}_{\text{edge}} = 0.5[|\log K_{+}(\text{int})| + |\log K_{-}(\text{int})|] \quad [15]$$

Estimates of PZC_{edge} based on Equation [15] were 8.42 for kaolinite, 8.16 for montmorillonite and 8.25 for illite. The effects of the permanent negative (interlayer) charge on phyllosilicates would effectively mask the PZC_{edge} and thus the overall PZC of the clay particle would be negative over most of the pH range. However, ions may

respond to the local charge at the particle edge and thus the PZC_{edge} may affect specifically adsorbing anions such as HAsO_4^{2-} , HPO_4^{2-} and MoO_4^{2-} .

Surface site densities (SOH_{T}) for the 3 clays are required input parameters for surface complexation modeling. Calculations of SOH_{T} using BET N_2 surface area and the suggested value of $2.31 \text{ sites nm}^{-2}$ (Davis and Kent 1990) were 3.5×10^{-5} for kaolinite, 7.1×10^{-5} for montmorillonite, and $9.3 \times 10^{-5} \text{ mol SOH g}^{-1}$ for illite. These values were 1 to 2 orders of magnitude higher than SOH_{T} obtained from experimentally measured maximum anion adsorption (As(V) + P adsorbed) in the binary As(V)/P systems. Therefore, values of SOH_{T} used for model optimizations for this study were calculated from anion adsorption envelopes measured as the sum of As(V) + P adsorbed at the pH of maximum adsorption (Table 1). These values

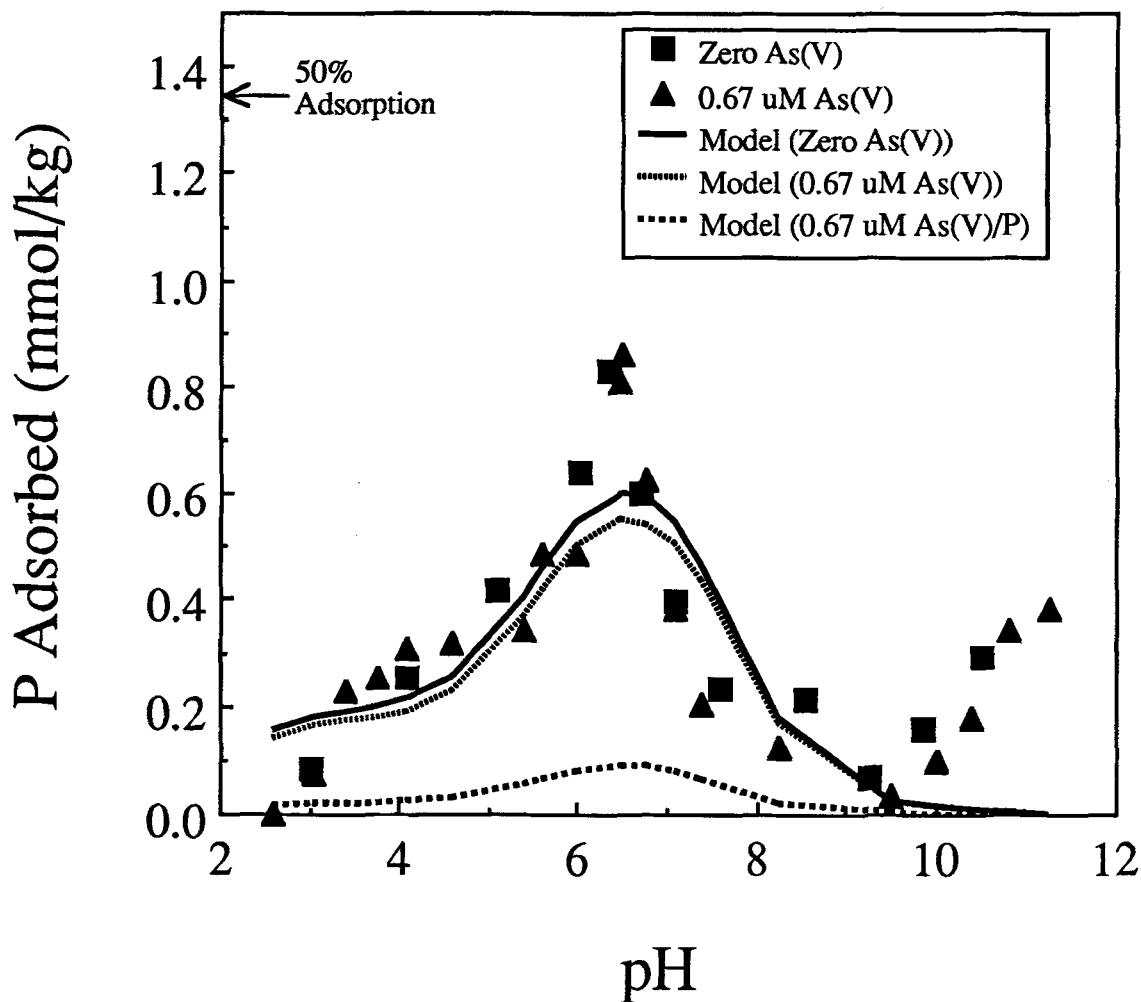


Figure 7. Experimental (points) and model (lines) P adsorption envelopes on illite (IMt-2) in the presence and absence of As(V). Five adjustable $K(\text{int})$ parameters were optimized to fit the CCM to single P anion data (solid line), whereas the $K(\text{int})$ values were held constant to predict competitive adsorption in binary systems (dotted lines). Reaction conditions: anion concentrations = $6.7 \mu\text{M P}/0.67 \mu\text{M As(V)}$ (binary system) or $6.7 \mu\text{M P}$ (single ion system), clay suspension density = 2.5 g L^{-1} , 0.1 M NaCl , and reaction time = 20 h. The lowest dashed line is a model prediction of P adsorption in the binary $0.67 \mu\text{M As(V)}/0.67 \mu\text{M P}$ system (no experimental data).

were more consistent with edge surface areas than with BET N_2 surface areas.

RESULTS AND DISCUSSIONS

As(V) and P Adsorption

Arsenate was rapidly adsorbed on the 3 clay minerals studied and the extent of As(V) adsorption remained nearly constant after 8 h (Figure 1). The pH of the suspensions was not controlled in this experiment and thus reflected ambient pH without addition of HCl or NaOH. Kinetic data for As(V) adsorption on clay minerals were not readily available in the literature, though kinetic data on P adsorption allowed indirect comparison. For example, Edzwald et al. (1976) showed a similar rapid adsorption of P on ka-

olinite, montmorillonite and illite. Chen et al. (1973b) reported a rapid (12 to 24 h) reaction of P with kaolinite followed by a slow process (1 to 60 d), that was attributed to slow nucleation and growth of a hexagonal AlPO_4 phase.

Arsenate adsorption on kaolinite was highly pH-dependent with a maximum between pH 4.7 and 6.0 and a steep decrease in adsorption between pH 6.3 and 7.5 (Figure 2). The PZC_{edge} of other kaolinites have been estimated to be 7.3 (Rand and Melton 1975) and 7.8 (Michaels and Bolger 1964), which would suggest that abrupt changes in electrostatic attraction between anions and the clay particle edge would occur in this pH region. The CCM gave an indirect and higher estimate of PZC_{edge} value for KGa-1 of 8.42 that was the

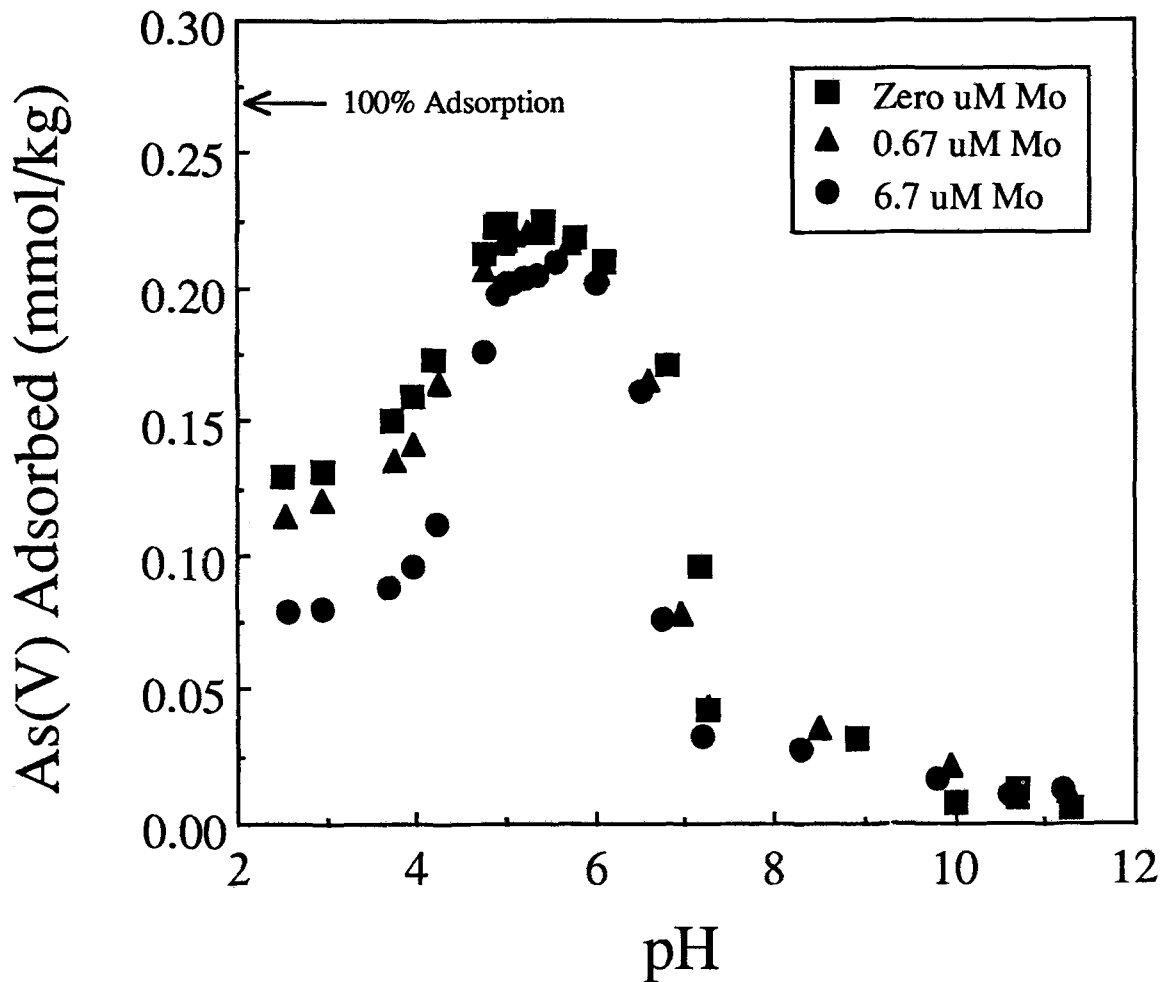


Figure 8. Experimental As(V) adsorption envelopes on kaolinite (KGa-1) at varying Mo concentrations. Initial As(V) concentration = $0.67 \mu\text{M}$, suspension density = 2.5 g L^{-1} , background electrolyte = 0.1 M NaCl , and reaction time = 20 h.

upper pH limit of the steep As(V) adsorption curve in Figure 2. The decline in As(V) adsorption on kaolinite below pH 4.7 (Figure 2) may be due to: 1) the dissolution of the kaolinite surface, which releases soluble Al^{3+} below pH 4.5 (Wieland and Stumm 1992), and subsequent $\text{AlH}_2\text{AsO}_4^{2+}$ or AlHAsO_4^+ complex formation; and/or 2) preferential adsorption of the H_2AsO_4^- species, which predominates between pH 3 and 7 (Frost and Griffin 1977).

The presence of 0.67 and $6.7 \mu\text{M P}$ decreased As(V) adsorption at pH 5 (the adsorption maximum) by 0.02 and $0.16 \text{ mmol kg}^{-1}$, respectively (Figure 2). The minor decrease (8.6%) in As(V) adsorption on kaolinite due to the presence of $0.67 \mu\text{M P}$ suggested that, at the adsorption maximum between pH 4 and 6, total anion (As(V)+P) adsorption on kaolinite in the binary As(V)/P system was greater than with As(V) alone. In the presence of 0.67 and $6.7 \mu\text{M P}$, the increased abundance of P in solution probably resulted in increased P at the available adsorption sites that displaced ad-

sorbed As(V). In contrast, Barrow (1992) investigated the co-adsorption of P and Se(IV) in a soil and concluded that competitive effects in dual P/Se(IV) adsorbate systems were due to surface charge modification caused by increased negative surface potential of soil colloids and not competition for adsorption sites. Therefore, surface charge modification may partially explain the net decrease in As(V) adsorption in binary As(V)/P systems.

The P adsorption envelope on kaolinite at $6.7 \mu\text{M P}$ starting concentration was similar to As(V) (Figure 3). Phosphate adsorption reached a maximum at pH 5 and declined abruptly at both higher and lower solution pH. Other investigations have reported P adsorption envelopes on kaolinite of a parabolic shape similar to As(V) with P adsorption maxima between pH 4 and 6 (Chen et al. 1973a; Edzwald et al. 1976). We did not measure simultaneous P adsorption in experiments with $0.67 \mu\text{M P} + 0.67 \mu\text{M As(V)}$ due to extremely low P concentrations ($<0.3 \mu\text{M P}$) in sample

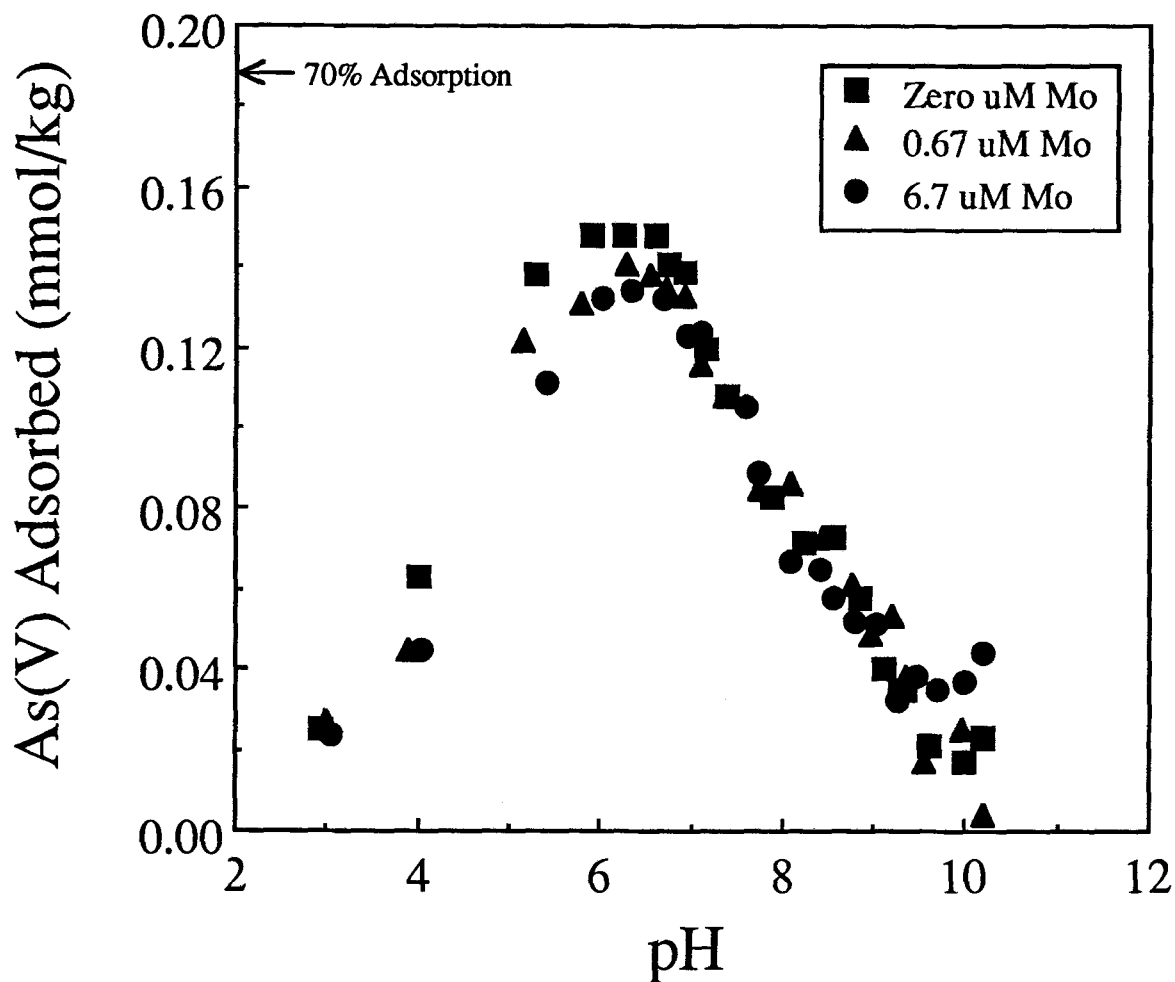


Figure 9. Experimental As(V) adsorption envelopes on montmorillonite (SWy-1) at varying Mo concentrations. Initial As(V) concentration = $0.67 \mu\text{M}$, suspension density = 2.5 g L^{-1} , background electrolyte = 0.1 M NaCl , and reaction time = 20 h.

solutions that were below the conductivity detection limit using ion chromatography. The competitive effect during co-adsorption from a binary solution of $6.7 \mu\text{M P} + 0.67 \mu\text{M As(V)}$ resulted in depressed As(V) adsorption (Figure 2). However, the presence of $0.67 \mu\text{M As(V)}$ had little effect on P adsorbed when P was present at the $6.7 \mu\text{M P}$ level (Figure 3).

Arsenate and P adsorption envelopes on montmorillonite are shown in Figures 4 and 5. The presence of $0.67 \mu\text{M P}$ caused a uniform decrease in the As(V)/montmorillonite adsorption envelope (Figure 4), whereas the presence of $0.67 \mu\text{M P}$ had little effect upon the As(V) adsorption envelope on illite (Figure 6). Increasing the P concentration to $6.7 \mu\text{M P}$ in dual As(V)/P adsorbate solutions decreased As(V) adsorption on kaolinite by 67%, montmorillonite by 47%, and illite by 82%, when measured at the pH values of the adsorption maxima. The presence of $6.7 \mu\text{M P}$ did not eliminate As(V) adsorption, indicating that even at relative As(V):P molar concentrations of 1:10, a frac-

tion of sites on phyllosilicates adsorbed As(V) with high specificity. The adsorption of P by montmorillonite (Figure 5) and illite (Figure 7) provided evidence that As(V) and P adsorb on these materials by similar mechanisms. Similarities in the pH of the As(V) and P adsorption maxima and the overall shapes of the adsorption envelopes, as well as competition for binding sites, suggested that the 2 anions bind to a similar suite of surface sites.

Maximum As(V) surface coverages on clays were between 0.11 to $0.21 \text{ mmol As(V) kg}^{-1}$. Muljadi et al. (1966) concluded that P adsorbs on kaolinite with high affinity when P surface coverage is less than 10 mmol kg^{-1} . Aluminum- and Fe (III)-hydroxy treated mica surfaces also exhibited 2 energetically distinct regions of P adsorption operating above and below P surface coverages of approximately $1 \times 10^{-6} \text{ mol m}^{-2}$ (Perrott et al. 1974). This implies that As(V)/P competitive adsorption in our experiments probably occurred on high affinity adsorption sites. Mineral surfaces contain fea-

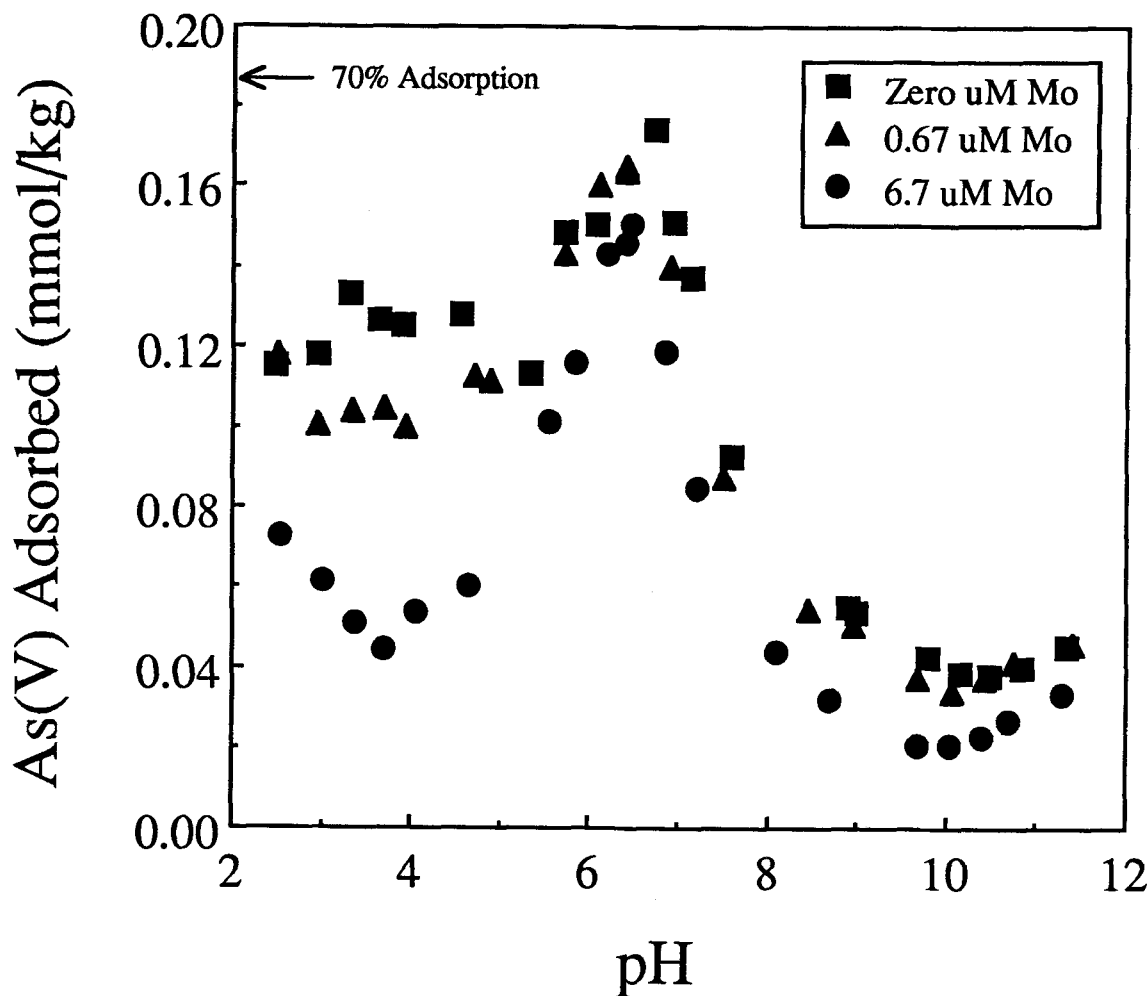


Figure 10. Experimental As(V) adsorption envelopes on illite (IMt-2) at varying Mo concentrations. Initial As(V) concentration = $0.67 \mu\text{M}$, suspension density = 2.5 g L^{-1} , background electrolyte = 0.1 M NaCl , and reaction time = 20 h.

tures such as kinks, steps and irregularly broken edges that will contribute to site heterogeneity and thus specific binding energies at different surface sites.

Modeling As(V) and P Competitive Adsorption

The results of applying the CCM to As(V) and P adsorption envelopes are indicated by lines in Figures 2 through 7. The optimized $\log K_{\text{As}}(\text{int})$ and $\log K_{\text{P}}(\text{int})$ values from single ion adsorption envelopes that were used to predict adsorption in binary systems are listed in Table 1. The FITEQL program converged readily on single ion data sets and these optimized model fits are indicated as solid lines in Figures 2 through 7. Preliminary work revealed that accurate model predictions of adsorption in binary As(V)/P systems depended on the magnitude of SOH_T used during single ion optimization of $K(\text{int})$ values. Therefore, optimized $K_{\text{As}}(\text{int})$ and $K_{\text{P}}(\text{int})$ values are system-specific and are

dependent on SOH_T , As(V) and P starting concentration and clay suspension density.

In the cases of kaolinite and illite, the model successfully predicted the minor decreases in As(V) adsorption in the presence of equimolar ($0.67 \mu\text{M}$) P (dotted lines, Figures 2 and 6). The model over-predicted As(V) adsorption on kaolinite and illite in $0.67/6.7 \mu\text{M}$ As(V)/P binary systems, though the shapes of the predicted envelopes are qualitatively accurate. The opposite scenario resulted from predictive modeling of As(V) adsorption on montmorillonite in the $0.67/6.7 \mu\text{M}$ As(V)/P binary system: the model underpredicted As(V) adsorption between pH 4 and 8 and gave a poorer qualitative agreement with the experimental envelope. Modeling of As(V) and P adsorption on kaolinite was limited to $\text{pH} > 4.75$ for 2 reasons: 1) the model did not readily converge on data over the entire pH range (2 to 11); and 2) mineral

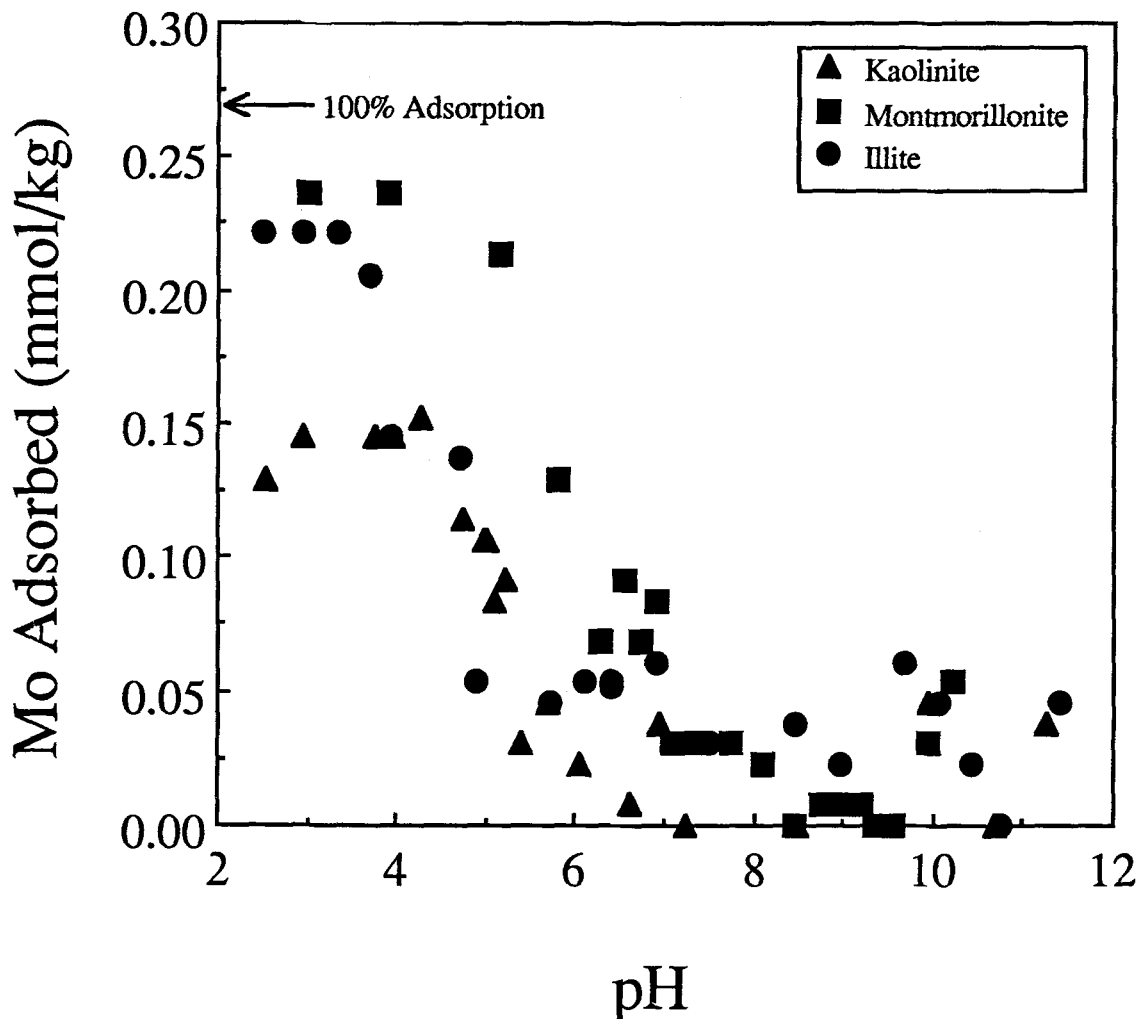


Figure 11. Experimental Mo adsorption envelopes on kaolinite (KGA-1), montmorillonite (SWy-1) and illite (IMt-2) during co-adsorption with As(V). Initial As(V) and Mo concentrations = $0.67 \mu\text{M}$, suspension density = 2.5 g L^{-1} , background electrolyte = 0.1 M NaCl , and reaction time = 20 h.

dissolution below pH 4.5 may invalidate the application of the model because of the possibility of As(V) solution complex formation. The FITEQL program converged readily on montmorillonite and illite As(V)/P single ion adsorption envelopes regardless of the pH region and thus, the entire pH range was modeled despite the possibility of dissolution.

Phosphate adsorption in $0.67/0.67 \mu\text{M}$ As(V)/P equimolar binary system was predicted based on $K_p(\text{int})$ values optimized in the $6.7 \mu\text{M}$ P systems. These simulations do not have experimental data for verification and are represented as the lower dotted lines in Figures 3, 5 and 7. Adsorbate surface coverages in the $0.67/0.67 \mu\text{M}$ As(V)/P systems were well below the estimated SOH_7 and hence, sites for adsorption were not limiting and minimal competition was predicted. Also included are model predictions of the

effect of $0.67 \mu\text{M}$ As(V) on $6.7 \mu\text{M}$ P adsorption (upper dotted lines in Figures 3, 5 and 7) that showed a modest depression in P adsorption that was not discernible in experimental data.

As(V) and Mo Adsorption

Arsenate adsorption envelopes on kaolinite, montmorillonite and illite generated in the presence of 0, 0.67, and $6.7 \mu\text{M}$ Mo are shown in Figures 8, 9 and 10, respectively. It was evident that the Mo anion (MoO_4^{2-}) did not substantially compete with As(V) for adsorption above pH 6. Below pH 6 the adsorption of As(V) on kaolinite and illite decreased due to competitive Mo adsorption. Only minor decreases in As(V) adsorption on montmorillonite due to Mo were measured. Analysis of Mo adsorption in the binary $0.67/0.67 \mu\text{M}$ As(V)/Mo system (Figure 11) showed

that Mo adsorption maxima on clays were at pH less than 4.5. The differentiation between the As(V) and Mo anions at clay mineral surfaces was revealed by the reversal in preferential adsorption from As(V) to Mo below pH 4 (kaolinite and illite) and pH 6 (montmorillonite). No attempts were made to apply the CCM to As(V) adsorption envelopes in Figures 8 through 10 because competition with Mo caused only minor decreases in As(V) adsorption at and above the pH of the adsorption maxima.

Differences between the adsorption behavior of As(V) and Mo on clays during simultaneous adsorption of the 2 anions are likely due to chemical differences (pK_a values, charge, ionic radii, polarizabilities, etc.). Chemical differences between As(V) and Mo anions could result in: 1) adsorption of As(V) and Mo at 2 distinct types of surface sites; 2) simultaneous adsorption of both As(V) and Mo on the same type of site at different pH; or 3) a combination of 1) and 2). This was in contrast to the similarities in pH-dependent adsorption behavior of the HAsO_4^{2-} and HPO_4^{2-} anions.

CONCLUSIONS

Arsenate adsorption was evaluated on 3 unpurified clay minerals (kaolinite, montmorillonite and illite) as a function final suspension pH and in the presence of P and Mo anions. Arsenate and P adsorption envelopes displayed similar adsorption maxima at pH 5.0 on kaolinite, at pH 6.0 on montmorillonite, and pH 6.5 on illite. Adsorption of As(V) and P declined steeply at $\text{pH} > 6.5$ in all clays. Arsenate adsorption on clay minerals decreased in the presence of P but was not substantially affected by the presence of Mo because substantial Mo adsorption did not occur at pH greater than 6.

Predicting anion competitive adsorption in whole soils will require a detailed understanding of the chemical reactions that occur at various mineral surfaces. The results of this study suggest that predicting As(V) adsorption in whole soil will be dependent upon soil solution pH and the presence of certain competing anions such as HPO_4^{2-} . Decreases in the amount of As(V) adsorption on clays due to P competition were generally described by the CCM at and above the pH of the As(V) adsorption maxima. The model allowed quantification of anion adsorption with capabilities for extending the application to systems of mixed anions.

More experimental work will be required to determine the chemical mechanism of oxyanion adsorption upon clay minerals. Determination of certain clay crystal edge properties such as edge surface site densities (SOH_+), direct measurement of the PZC_{edge} , the relationship between conventional surface area measurements and the edge surface area and the effects of permanent negative charge of the particle on edge site adsorption, will all be necessary for a complete un-

derstanding of the adsorption of oxyanions on clay minerals. To better predict ion adsorption on mineral surfaces with surface complexation models using a minimum number of adjustable parameters, more detailed information about reactive adsorption sites will be required.

ACKNOWLEDGMENT

We gratefully acknowledge H. Forster of the U.S. Salinity Laboratory for assistance with XRD analyses.

REFERENCES

- Anderson MA, Malotky DT. 1979. The adsorption of polyzable anions on hydrous oxides at the isoelectric pH. *J Coll Interface Sci* 72:413–427.
- Barrow NJ. 1992. The effect of time on the competition between anions for sorption. *J Soil Sci* 43:421–428.
- Bleam WF, Pfeffer PE, Goldberg S, Taylor RW, Dudley R. 1991. A ^{31}P solid-state nuclear magnetic resonance study of phosphate adsorption at the boehmite/aqueous solution interface. *Langmuir* 7:1702–1712.
- Chen YSR, Butler JN, Stumm W. 1973a. Adsorption of phosphate on alumina and kaolinite from dilute aqueous solutions. *J Coll Interface Sci* 43:421–436.
- Chen YSR, Butler JN, Stumm W. 1973b. Kinetic study of phosphate reaction with aluminum oxide and kaolinite. *Environ Sci Technol* 7:327–332.
- Davis JA, Kent DB. 1990. Surface complexation modeling in aqueous geochemistry. *Rev Mineral* 23:177–260.
- Edzward JK, Toensing DC, Leung MCY. 1976. Phosphate adsorption reactions with clay minerals. *Environ Sci Technol* 10:485–490.
- Ferguson JF, Gavis J. 1972. A review of the arsenic cycle in natural waters. *Water Res* 6:1259–1274.
- Frost RR, Griffin RA. 1977. Effect of pH on adsorption of arsenic and selenium from landfill leachate by clay minerals. *Soil Sci Soc Am J* 41:53–57.
- Glaubig RA, Goldberg S. 1988. Determination of inorganic arsenic (III) and arsenic (III plus V) using automated hydride-generation atomic-absorption spectrometry. *Soil Sci Soc Am J* 52:536–537.
- Goldberg S. 1986. Chemical modeling of arsenate adsorption on aluminum and iron oxide minerals. *Soil Sci Soc Am J* 50:1154–1157.
- Goldberg S, Glaubig RA. 1988. Anion sorption on a calcareous, montmorillonitic soil-arsenic. *Soil Sci Soc Am J* 52:1297–1300.
- Herbelin AL, Westall JC. 1994. FITEQL: A computer program for the determination of chemical equilibrium constants from experimental data. Rep. 94-01, Oregon State University, Corvallis.
- Hingston FJ, Posner AM, Quirk JP. 1971. Competitive adsorption of negatively charged ligands on oxide surfaces. *Discuss Faraday Soc* 52:334–342.
- Hingston FJ, Posner AM, Quirk JP. 1972. Anion adsorption by goethite and gibbsite. I. The role of the proton in determining adsorption envelopes. *J Soil Sci* 23:177–192.
- Hsia TH, Lo SL, Lin CF, Lee DY. 1994. Characterization of arsenate adsorption on hydrous iron oxide using chemical and physical methods. *Colloids Surf A: Physicochemical and Engineering Aspects* 85:1–7.
- Huang PM. 1975. Retention of arsenic by hydroxy-aluminum on surfaces of micaceous mineral colloids. *Soil Sci Soc Am Proc* 39:271–274.
- Jacobs LW, Syers JK, Kenney DR. 1970. Arsenic sorption by soils. *Soil Sci Soc Am Proc* 34:750–754.

- Keren R, Talpaz H. 1984. Boron adsorption by montmorillonite as affected by particle size. *Soil Sci Soc Am J* 48: 555–559.
- Livesey NT, Huang PM. 1981. Adsorption of arsenate by soils and its relation to selected chemical properties and anions. *Soil Sci* 131:88–94.
- Lumsdon DG, Fraser AR, Russell JD, Livesey NT. 1984. New infrared band assignments for the arsenate ion adsorbed on synthetic goethite. *J Soil Sci* 35:381–386.
- Manning BA, Goldberg S. 1996. Modeling competitive adsorption of arsenate with phosphate and molybdate on oxide minerals. *Soil Sci Soc Am J* 60:121–131.
- Masscheleyn PH, Delaune RD, Patrick WH Jr. 1991a. Effect of redox potential and pH on arsenic speciation and solubility in a contaminated soil. *Environ Sci Technol* 25:1414–1419.
- Masscheleyn PH, Delaune RD, Patrick WH Jr. 1991b. Arsenic and selenium chemistry as affected by sediment redox potential and pH. *J Environ Qual* 20:522–527.
- Michaels AS, Bolger JC. 1964. Particle interactions in aqueous kaolinite suspensions. *Ind Eng Chem Fundam* 3:14–20.
- Motta MM, Miranda CF. 1989. Molybdate adsorption on kaolinite, montmorillonite, and illite: Constant capacitance modeling. *Soil Sci Soc Am J* 53:380–385.
- Muljadi D, Posner AM, Quirk JP. 1966. The mechanism of phosphate adsorption on kaolinite, gibbsite and pseudo-boehmite. I. The isotherms and the effect of pH on adsorption. *J Soil Sci* 17:212–229.
- Perrott KW, Langdon AG, Wilson AT. 1974. Sorption of phosphate by aluminum and iron(III)-hydroxy species on mica surfaces. *Geoderma* 12:223–231.
- Rand B, Melton JE. 1975. Isoelectric point of the edge surface of kaolinite. *Nature* 257:214–216.
- Roy WR, Hassett JJ, Griffin RA. 1986. Competitive coefficients for the adsorption of arsenate, molybdate, and phosphate mixtures by soils. *Soil Sci Soc Am J* 50:1176–1182.
- Sadiq M, Zaida TH, Mian AA. 1983. Environmental behavior of arsenic in soils: Theoretical. *Water Air Soil Pollut* 20:369–377.
- Schindler PW, Gamsjäger H. 1972. Acid-base reactions of the TiO₂ (anatase)-water interface and the point of zero charge of TiO₂ suspensions. *Kolloid Z Z Polym* 250:759–763.
- Stumm W, Hohl H, Dalang F. 1976. Interactions of metal ions with hydrous oxide surfaces. *Croat Chem Acta* 48: 491–504.
- Stumm W, Huang CP, Jenkins SR. 1970. Specific chemical interaction affecting the stability of dispersed systems. *Croat Chem Acta* 42:223–245.
- Stumm W, Kummert R, Sigg L. 1980. A ligand exchange model for the adsorption of inorganic and organic ligands at hydrous oxide interfaces. *Croat Chem Acta* 53:291–312.
- Swartzen-Allen LS, Matijevic E. 1974. Surface and colloid chemistry of clays. *Chem Rev* 74:385–400.
- Waychunas GA, Rea BA, Fuller CC, Davis JA. 1993. Surface chemistry of ferrihydrite: Part 1. EXAFS studies of the geometry of coprecipitated and adsorbed arsenate. *Geochim Cosmochim Acta* 57:2251–2269.
- Westall JC, Hohl H. 1980. A comparison of electrostatic models for the oxide/solution interface. *Adv Coll Interface Sci* 12:265–294.
- Wieland E, Stumm W. 1992. Dissolution kinetics of kaolinite in acidic aqueous solutions at 25°C. *Geochim Cosmochim Acta* 56:3339–3355.
- Xu H, Allard B, Grimvall A. 1988. Influence of pH and organic substance on the adsorption of As(V) on geologic materials. *Water Air Soil Pollut* 40:293–305.
- Zachara JM, Cowan CE, Schmidt RL, Ainsworth CC. 1988. Chromate adsorption by kaolinite. *Clays Clay Miner* 36: 317–326.

(Received 29 June 1995; accepted 20 December 1995; Ms. 2664)